

Instability of dilute granular flows on rough slope

Namiko MITARAI* and Hiizu NAKANISHI**

Department of Physics, Kyushu University 33, Fukuoka 812-8581

(Received November 21, 2018)

We study numerically the stability of granular flow on a rough slope in collisional flow regime in the two-dimension. We examine the density dependence of the flowing behavior in low density region, and demonstrate that the particle collisions stabilize the steady flow above a certain density in the parameter region where a single particle would show an accelerated behavior. Within this collisional steady flow regime, however, the uniform steady flow is only metastable and is shown to be unstable against clustering when the particle density is not high enough.

KEYWORDS: granular flow, surface flow, clustering, inelastic collision, simulation, discrete element method

Granular flow on a slope is one of the simplest situations to see the characteristic behavior of granular dynamics. When the inclination angle is smaller than a certain value (the angle of repose), the material never flows because of the stress sustained by the friction. Beyond that angle, the surface layers of the material begin to flow like a fluid, but the bottom part of the materials may remain solidified when the inclination angle is not steep enough.¹⁾ If the inclination is increased further, all of the material starts to flow rapidly, and the interaction between particles or between a particle and the slope is dominated by the inelastic collision, rather than friction.

Many researches have been done in such a collisional flow regime, but most of them focus on the property of the steady uniform flow.^{2,3,4)} In such researches, the depth dependence of the flow properties such as velocity or density profile is investigated, assuming that the flow is uniform in the direction along the slope. It is known, however, that the granular materials have the tendency to cluster due to the inelastic collision, which causes the formation of density waves in the case of granular flow in a vertical pipe.^{6,5)} Therefore, it is natural to expect that this tendency will cause some instability in uniform flow on a slope.

Granular flow of an independent particle, or a single particle behavior, has been studied, and has been found to show three types of motion depending on the inclination angle and roughness of the slope.^{7,8,9)} For the fixed roughness of the slope, the following behaviors are observed upon increasing the inclination angle: (i)The particle stops after a few collisions with the slope for any initial velocity (regime A). (ii)The particle quickly reaches a constant averaged velocity in the direction along the slope and shows almost steady motion; the averaged velocity does not depend on the initial condition (regime B). (iii)The particle jumps and accelerates as it goes down the slope (regime C).

In the present work, we study how the above single particle picture will be modified in the collisional flow

with finite density by the particle collisions. Based on numerical simulations, we determine the parameter region where the steady flow is realized with the finite density, and examine the stability of the uniform flow.

We employed the discrete element method^{10,11)} with the normal and the tangential elastic force and dissipation. In the simulations, granular particles are modeled by two-dimensional disks with mass m and diameter d . When the two disks i and j at positions \mathbf{r}_i and \mathbf{r}_j with velocities \mathbf{v}_i and \mathbf{v}_j and angular velocities ω_i and ω_j are in contact, the force acting on the particle i from the particle j is calculated as follows: The normal velocity v_n , the tangential velocity v_t , and the tangential displacement u_t are given by

$$v_n = \mathbf{v}_{ij} \cdot \mathbf{n}, \quad v_t = \mathbf{v}_{ij} \cdot \mathbf{t} - (d/2)(\omega_i + \omega_j), \quad (1)$$

$$u_t = \int_{t_0}^t v_t dt, \quad (2)$$

with the normal vector $\mathbf{n} = \mathbf{r}_{ij}/|\mathbf{r}_{ij}| = (n_x, n_y)$ and the tangential vector $\mathbf{t} = (-n_y, n_x)$. Here, $\mathbf{r}_{ij} = \mathbf{r}_j - \mathbf{r}_i$, $\mathbf{v}_{ij} = \mathbf{v}_j - \mathbf{v}_i$, and t_0 is the time when the particles started to contact. Then the normal force F_{ij}^n and the tangential force F_{ij}^t acting on the particle i from the particle j are given by

$$F_{ij}^n = -k_n(d - |\mathbf{r}_{ij}|) + \eta_n v_n, \quad (3)$$

$$F_{ij}^t = \min(|h_t|, \mu |F_{ij}^n|) \text{sign}(h_t) \quad (4)$$

with $h_t = k_t u_t + \eta_t v_t$, where k_n and k_t are elastic constants, η_n and η_t are damping parameters, and μ is the Coulomb friction coefficient for sliding friction. Each particle is also subject to the gravity, and the gravitational acceleration is given by $\mathbf{g} = g(\sin \theta, -\cos \theta)$. The surface of the slope is made rough by gluing the particles identical with the moving ones with spacing $2\epsilon d$ with $\epsilon = 0.001$ (Fig. 1). The periodic boundary condition is imposed in the x direction. The system size L is determined by the number of the particles glued on the slope n_s as $L = (1 + 2\epsilon)dn_s$.

All quantities which appear in the following are given in the non-dimensionalized form in terms of the length

* E-mail: namiko@stat.phys.kyushu-u.ac.jp

** E-mail: naka4sep@mbox.nc.kyushu-u.ac.jp

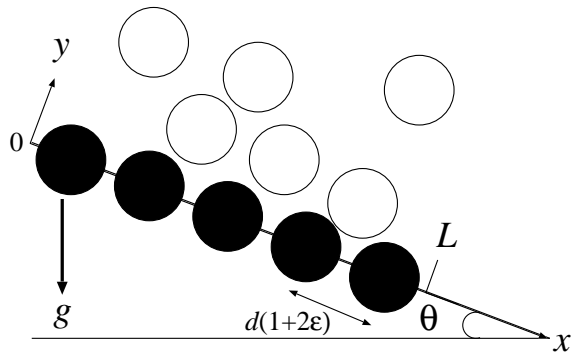


Fig. 1. A schematic illustration of the system geometry.

Table I. Parameters used in the simulations.

k_n	k_t	η_n	η_t	μ
5×10^4	$(5 \times 10^4)/3$	35.68	$35.68/3$	0.5

unit d , the mass unit m , and the time unit $\tau = (d/g)^{1/2}$. The parameters used in the simulations are tabulated in Table I. With these parameters, the normal restitution coefficient (the ratio of normal relative velocities of pre- and post-collision) e_n turns out to be around 0.7. We integrated the equations of motions using the predictor-corrector method in the third order with constant time step $\delta t = 1 \times 10^{-4}$.

We first investigate how the steady flow appears when we increase the density of flowing particles from one particle limit.

As we have referred, a particle on a slope shows three types of behavior depending on the value of θ . It is known, however, that the boundary between the regime B (the constant velocity regime) and C (the acceleration regime) is not sharp; there is a parameter region where the particle can attain steady state or can accelerate, depending on the initial condition. We should also note that, when the initial kinetic energy of the particle is too small, the particle may stop in the regime B and in part of the regime C. In the present model with the parameters in Table I, it turns out that the regime A roughly corresponds to the region $\sin \theta \lesssim 0.11$, the regime B to $0.11 \lesssim \sin \theta \lesssim 0.14$, and the regime C to $0.16 \lesssim \sin \theta$.

Now we focus on what happens when the number of moving particles n is increased with the finite L . It is easy to expect that the dissipation becomes larger upon increasing n , because the collisions between particles or a particle and the slope become more frequent. Therefore it is obvious that, if θ is in the regime A, then all the particles will stop irrespective of the initial condition. Even for the θ in the regime B, it turns out that the collisions between particles eventually stop all the particles.

We examine closely the flowing behavior for the larger inclination angle θ that is in the regime C. The situation is presented by showing the simulations with $\sin \theta = 0.45$

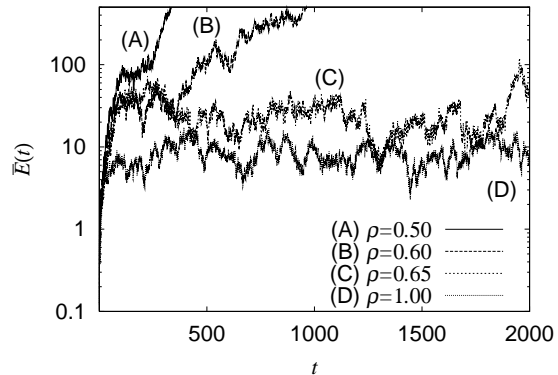


Fig. 2. The semi-log plot of $\bar{E}(t)$ for $\rho = 0.50, 0.60, 0.65$, and 1.00 , with $\sin \theta = 0.45$ and $L = 20.04$. $\bar{E}(t)$ continues to grow when $\rho \leq 0.60$, while it is bounded when $\rho \geq 0.65$.

and $L = 20.04$. We set the initial condition as follows:

$$x_i(0) = (L/n)(i-1), \quad y_i(0) = (1+2\epsilon)d + 3\xi_i, \quad (5)$$

$$u_i(0) = 0, \quad v_i(0) = 0, \quad \omega_i(0) = 0, \quad (6)$$

where $x_i(t)$ ($y_i(t)$) and $u_i(t)$ ($v_i(t)$) are the coordinate and the velocity of center of mass of the i th particle at time t in the x (y) direction, respectively. ξ_i is a random number uniformly distributed over the interval $[0, 1]$. In the following, we define the 'density' of the particles as $\rho = n/L$. In order to characterize the qualitative difference of accelerated behavior in the regime C and the steady collisional flow, we investigate the ρ dependence of the averaged kinetic energy $\bar{E}(t)$ defined as

$$\bar{E}(t) = \frac{1}{n} \sum_{i=1}^n E_i(t), \quad (7)$$

where $E_i(t)$ is the kinetic energy of the i th particle at time t ;

$$E_i(t) = \frac{1}{2}m [u_i(t)^2 + v_i(t)^2] + \frac{1}{2}I\omega_i(t)^2, \quad (8)$$

with $I = md^2/8$.

In Fig. 2, the time evolutions of $\bar{E}(t)$ are shown for several values of ρ . When ρ is small ($\rho \leq 0.60$), $\bar{E}(t)$ grows rapidly, but the growth rate becomes smaller as ρ increases. In this region, each particle jumps and rarely collides with each other. When $\rho \geq 0.65$, $\bar{E}(t)$ still grows rapidly in early stage, but its long-time behavior seems to be bounded and fluctuate around a constant value. In this case each particle also jumps, but often collides with other particles and is prevented from jumping up infinitely. Based on this observation, we define the steady flow in the low-density limit as the flow where the value of $\bar{E}(t)$ is bounded over a long time. Figure 3 shows the 'phase diagram' summarizing the behavior in terms of θ and ρ . In order to obtain the diagram, 10 simulations with $L = 20.04$ were done for each θ and ρ until $t = 2000$. When $\bar{E}(t)$ never exceeds 500 in the simulation but still has a non-zero finite value, we judge that the steady flow is realized. It should be noted that, even within the parameter region shown in Fig. 3, all the particles may

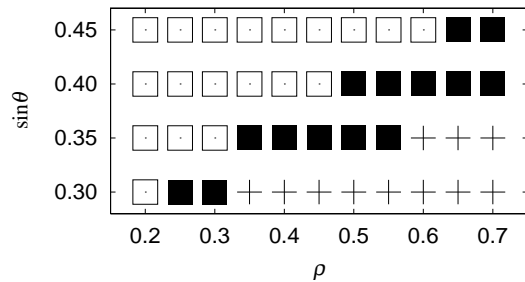


Fig. 3. The ‘phase diagram’ obtained from the simulations with $L = 20.04$. The accelerated regime (open box), the steady flow regime (filled box), and the regime where all the particles stop (plus) are shown when more than 50 % of trials result in the corresponding behavior.

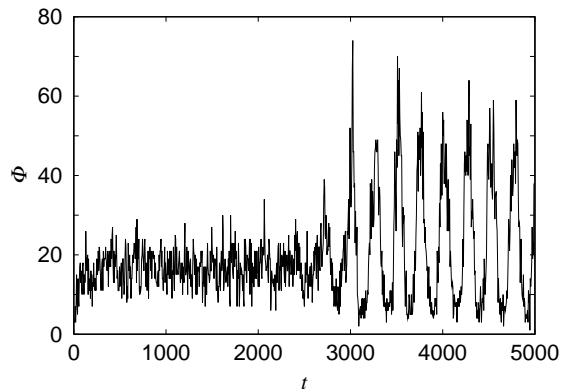


Fig. 4. The time evolution of the flux $\Phi(t)$ in the simulation with $L = 1002$ and $\rho = 1.0$. A fluctuation grows to form a cluster spontaneously.

stop ($\bar{E}(t)$ becomes zero). Namely we can see three types of behavior; (i) accelerated motion, (ii) steady flow, (iii) static state where all the particles come to rest. Each point in Fig. 3 is determined to be in one of these regimes if more than 50 % of the trials show the corresponding behavior.

Now we examine the stability of the uniform collisional flow. First we show the simulation results of the flow in the system with $\sin \theta = 0.45$, $L = 1002$ and $n = 1000$, i.e. $\rho = 1.0$. Figure 4 shows the time evolution of the flux $\Phi(t)$ defined as the number of the particles which pass $x = L/2$ during the time interval $\Delta t = 10$. In early stage the flux is almost steady ($300 \lesssim t \lesssim 2000$), namely uniform steady flow is realized. Then $\Phi(t)$ shows large fluctuation which grows in the course of time ($2000 \lesssim t \lesssim 3000$); this means the clustering behavior is triggered by the fluctuation. Finally $\Phi(t)$ begins to oscillate almost periodically with large amplitude ($t \gtrsim 3000$). This oscillation of the flux indicates that one large cluster of particles travels in the system with almost constant velocity; we can see that the cluster is stable once it is formed.

In Figs. 5, the time evolutions of (a) the averaged kinetic energy $\bar{E}(t)$ and (b) the kinetic energy of a particular particle $E_1(t)$ are also shown. Both of them are al-

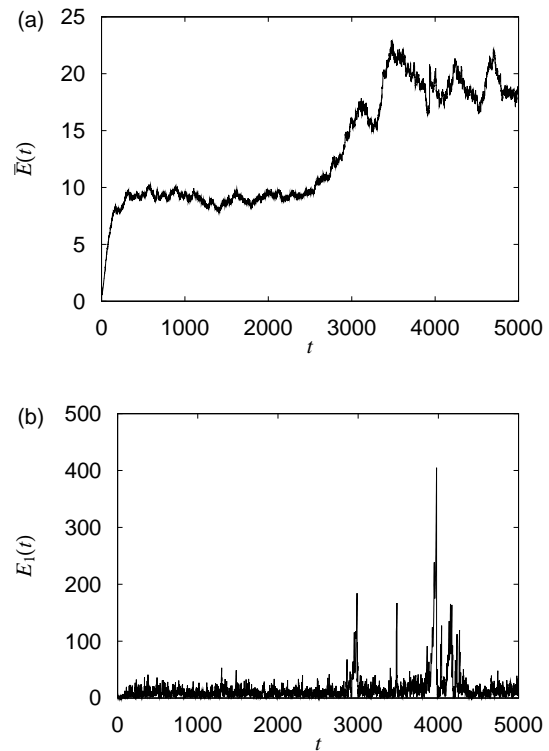


Fig. 5. The time evolution of (a) $\bar{E}(t)$ and (b) $E_1(t)$ in the simulation with $L = 1002$ and $\rho = 1.0$. Compared with Fig. 4, we can see that, after the clustering occurs ($t \gtrsim 3000$), the time averaged value of $\bar{E}(t)$ becomes larger than that in the uniform flow stage, and $E_1(t)$ begins to show large fluctuation.

most constant in the stage of uniform steady flow. Then $\bar{E}(t)$ increases in $2000 \lesssim t \lesssim 3000$. In $t \gtrsim 3000$, the fluctuation of $E_1(t)$ becomes considerably large, and $\bar{E}(t)$ begins to fluctuate around another constant value which is larger than the one in the stage of uniform flow. The reason why the kinetic energy increases when a cluster is formed can be understood as follows: When the cluster is formed, the region with the density lower than the threshold value to maintain the steady flow (~ 0.65 in the case of $\sin \theta = 0.45$, see Fig. 3.) appears locally, and particles in such a spatial region can be highly accelerated. However, the particle will be caught in the cluster sooner or later, and then quickly lose its kinetic energy. This mechanism maintains the moving cluster, and results in the large fluctuations in $E_1(t)$.

In order to examine the system size and the density dependence of the clustering, the time evolutions of the flux for a few values of densities with $L = 501$ are also shown in Figs. 6. Figure 6 (a) shows the result with $\rho = 1.0$ ($n = 500$), which is the same density as the simulation in Fig. 4. However, no clustering behavior can be seen clearly in Fig. 6 (a), even though the fluctuation is very large. We have also simulated in the system with $L = 250.05$ and $\rho = 1.0$ ($n = 250$), but the clustering behavior was not found, either. On the other hand, Figs. 6 (b) and (c) are the results with $\rho = 2.0$ ($n = 1000$) and $\rho = 0.75$ ($n = 375$), respectively. It is found that the uniform flow is maintained in Fig. 6 (b), while the clear

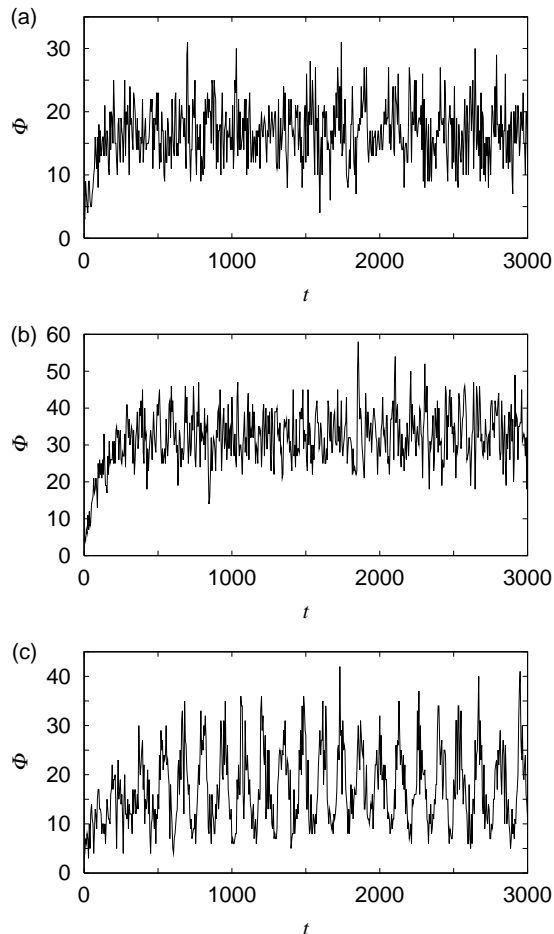


Fig. 6. The time evolution of the flux $\Phi(t)$ in the simulation with $L = 501$ and (a) $\rho = 1.0$, (b) $\rho = 2.0$, and (c) $\rho = 0.75$.

oscillation of the flux associated with the cluster formation is seen in Fig. 6 (c). From these results, we can see the general tendency that the uniform flow tends to be stabilized as the system size is smaller or as the density is higher.

In summary, we have examined the two-dimensional granular flow on a rough slope in the collisional flow regime by numerical simulations. It was shown that the mutual collisions among particles stabilizes the steady flow even in the accelerated regime for a single particle system. The phase diagram was determined for the accelerated, steady, and stopping regime in terms of the particle density ρ and the inclination angle θ for a particular system size. The stability of uniform steady flow was also examined and we found that a large single cluster appears spontaneously out of a uniform initial state. It was shown that the smaller the particle density is, or the larger the system size is, the less stable the uniform steady flow is.

Before concluding, let us make a comment on the system size dependence of the instability. We also simulated the system with $L = 501$ and $\rho = 1.0$ with the initial configuration with large inhomogeneity along the flow direction. Then it was found that a cluster is formed after a while, but it is broken when the head and the tail of the cluster collide through the periodic boundary condition.

When the density is the same, the size of sparse region is larger for a larger system, while the fluctuation around the edge of the cluster is determined mainly by the local configuration. Therefore, a cluster will be stabler when the system size is larger. It is still a future issue to clarify the detailed mechanism how the system size and the density affect the instability.

Part of the computation in this work has been done using the facilities of the Supercomputer Center, Institute for Solid State Physics, University of Tokyo.

-
- [1] H. M. Jaeger, S. R. Nagel and R. P. Behringer: *Rev. Mod. Phys.* **68** (1996) 1259.
 - [2] T. G. Drake: *J. Fluid. Mech.* **225** (1991) 121.
 - [3] T. Pöschel: *J. Phys. II (France)* **3** (1993) 27.
 - [4] E. Azanza, F. Chevoir, and P. Moucheront: *J. Fluid. Mech.* **400** (1999) 199.
 - [5] J. Lee: *Phys. Rev. E* **49** (1994) 281.
 - [6] S. Horikawa, A. Nakahara, T. Nakayama, and M. Matsushita: *J. Phys. Soc. Jpn.* **64** (1995) 1870.
 - [7] F.-X. Rigidel, R. Jullien, G. H. Ristow, A. Hansen, and D. Bideau: *J. Phys. I (France)* **4** (1994) 261.
 - [8] G. H. Ristow, F.-X. Rigidel, and D. Bideau: *J. Phys. I (France)* **4** (1994) 1161.
 - [9] S. Dippel, G. Batrouni, and D. E. Wolf: *Phys. Rev. E* **54** (1996) 6845.
 - [10] P. A. Cundall and O. D. L. Strack: *Geotechnique* **29** (1979) 47.
 - [11] A. Shimosaka: *Funtai Simulation Nyumon* (Introduction to Simulations of Granular Materials), ed. The Society of Powder Technology, Japan (Sangyo Tosho, Tokyo, 1998) Sec. 3.2, p. 34 [in Japanese].